# Modifying the Interaction Parameters of a Linear ABC Triblock Terpolymer by Functionalizing the Short, Reactive Middle Block to Induce Morphological Change

Kevin Wylie, Lei Dong, Alvin Chandra, Yuta Nabae, Teruaki Hayakawa*

Department of Materials Science and Engineering, School of Materials and Chemical Technology, Tokyo Institute of Technology, 2-12-1-S8-36 Ookayama, Meguro-ku, Tokyo 152-8552, Japan
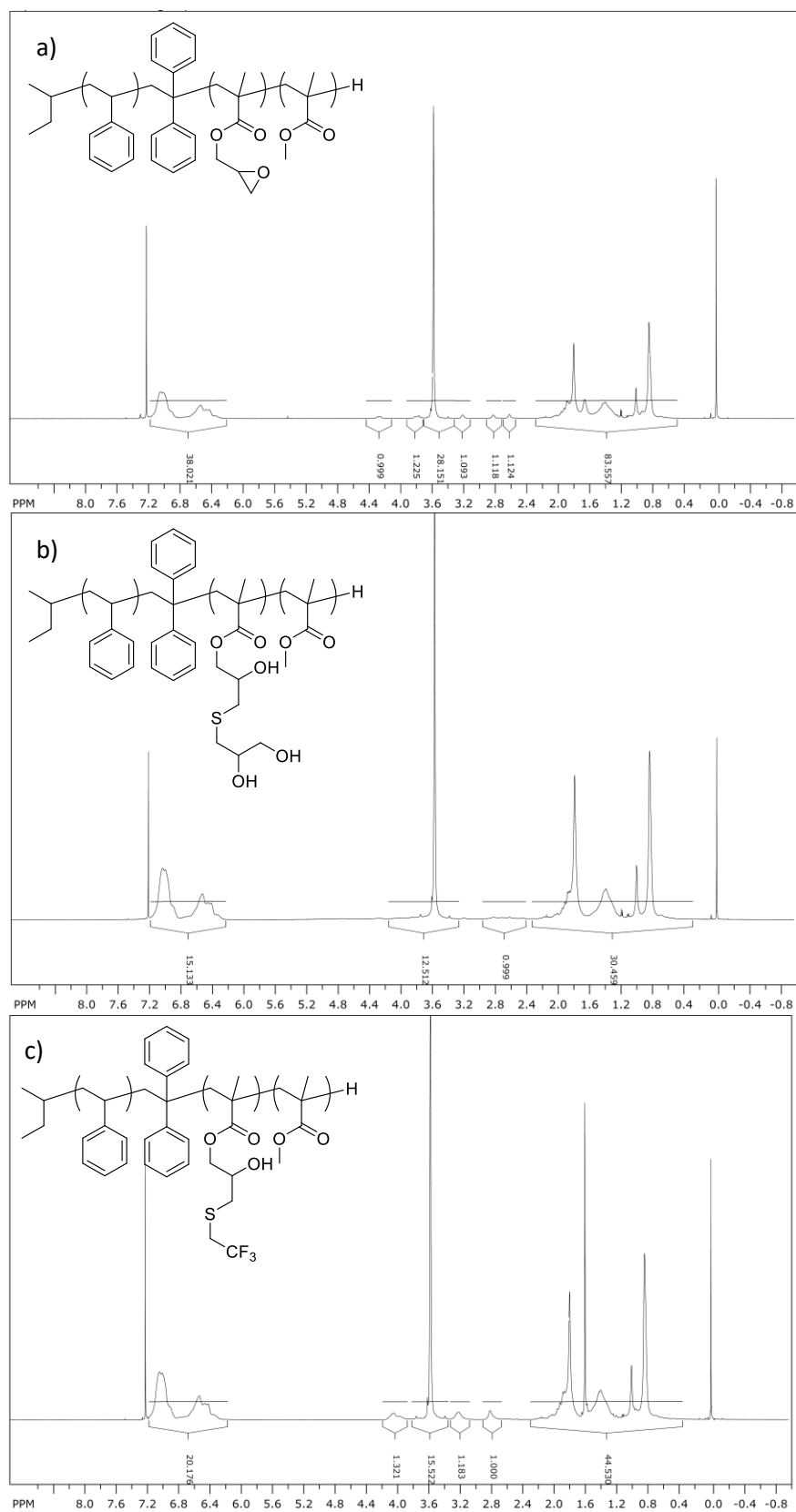
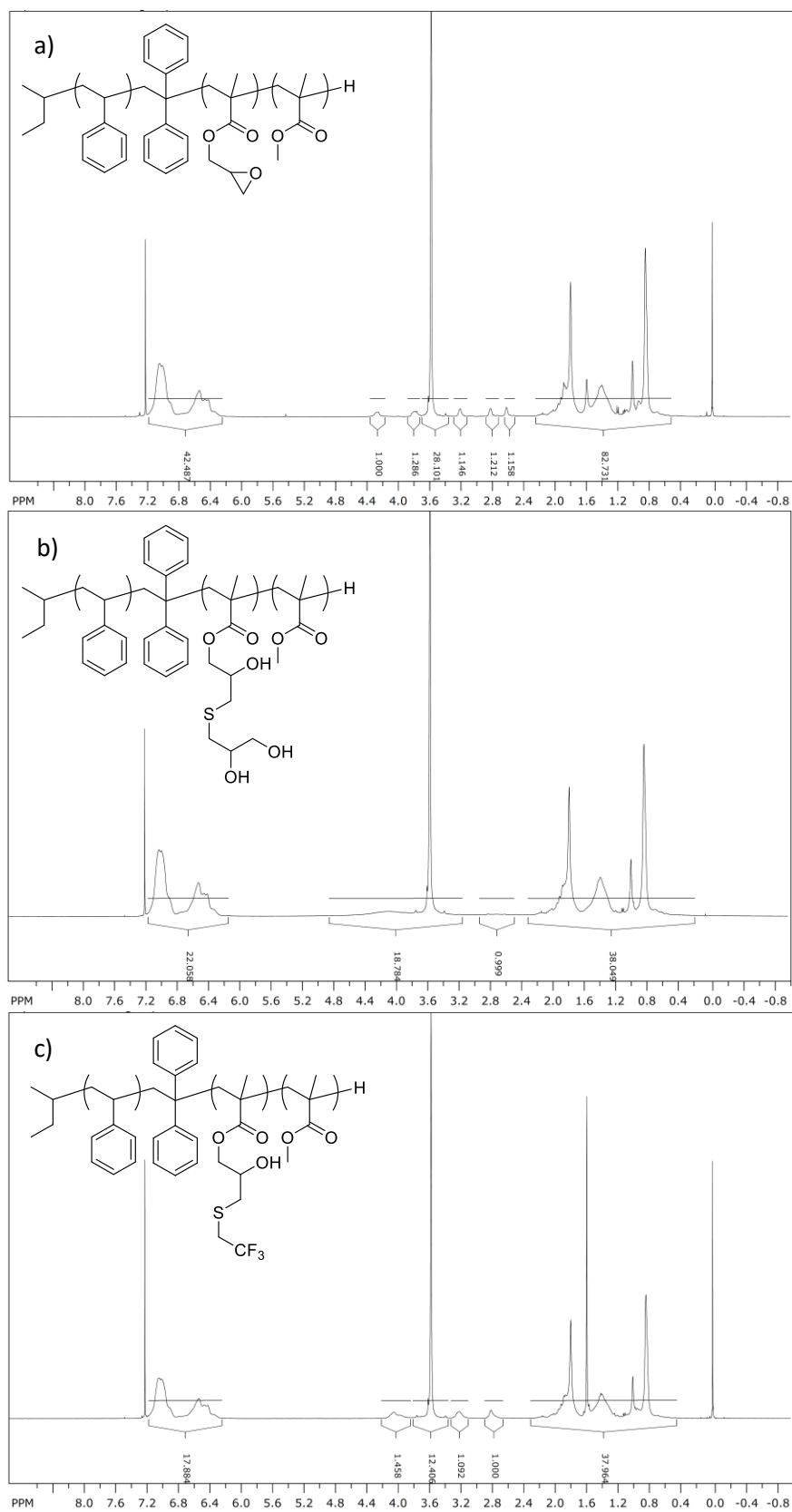**Figure S1.** $^1$H NMR spectra of a) PSGM21, b) PSGM21$_{OH}$, and c) PSGM21$_F$ in CDCl$_3$.

**Figure S2.** $^{1}$H NMR spectra of a) PSGM18, b) PSGM18$_{OH}$, and c) PSGM18$_F$ in CDCl$_3$.

**Figure S3.** $^1$H NMR spectra of a) PSGM15, b) PSGM15$_{OH}$, and c) PSGM15$_F$ in CDCl$_3$.
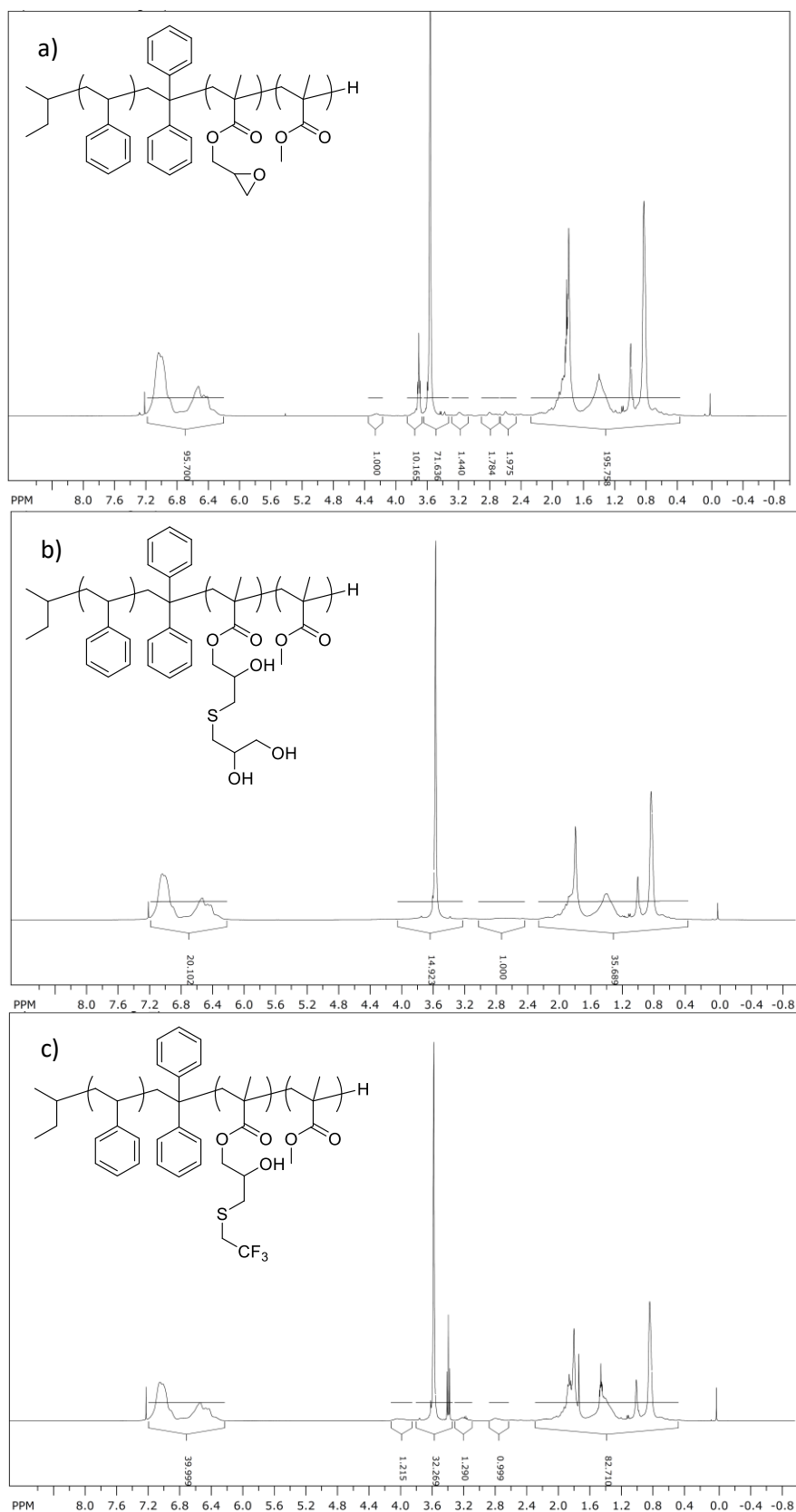
**Figure S4.** $^1$H NMR spectra of a) PSGM10, b) PSGM10$_{OH}$, and c) PSGM10$_F$ in CDCl$_3$.

PSGM$_{OH}$ samples were measured on a Viscotek GPC-1000 system equipped with a TDA 302 triple detector (Malvern Instruments Ltd., UK) and a TSKgel α-M column (Tosoh Corp., Japan) with *N,N*-dimethylformamide (DMF) containing 0.05 M lithium bromide as the eluent at 313 K.
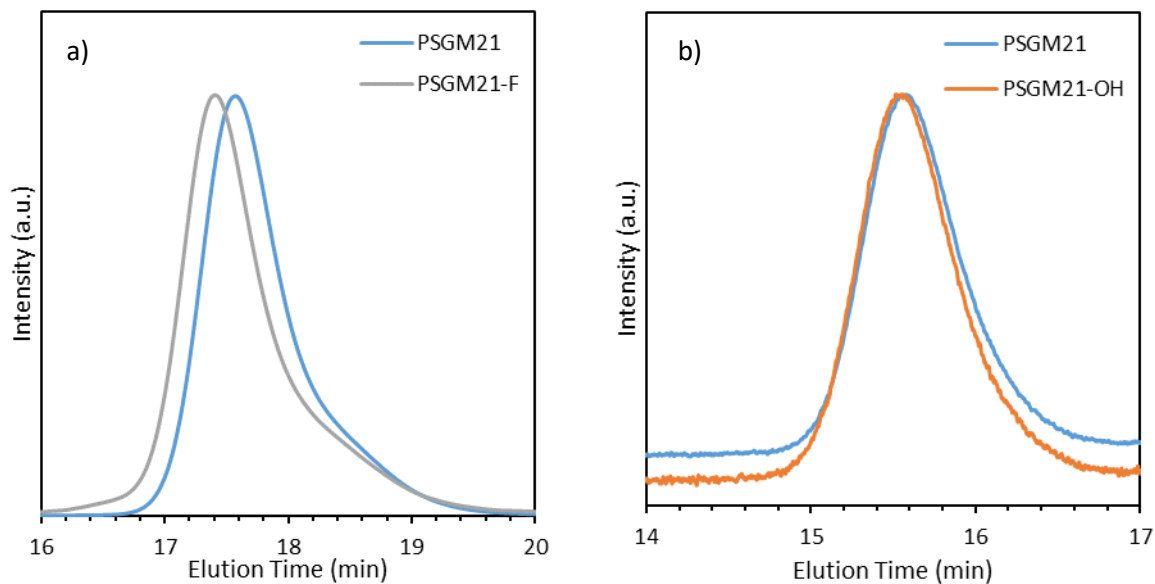


**Figure S5.** SEC traces of a) PSGM21 and PSGM21$_F$ in THF and b) PSGM21 and PSGM21$_{OH}$ in DMF.
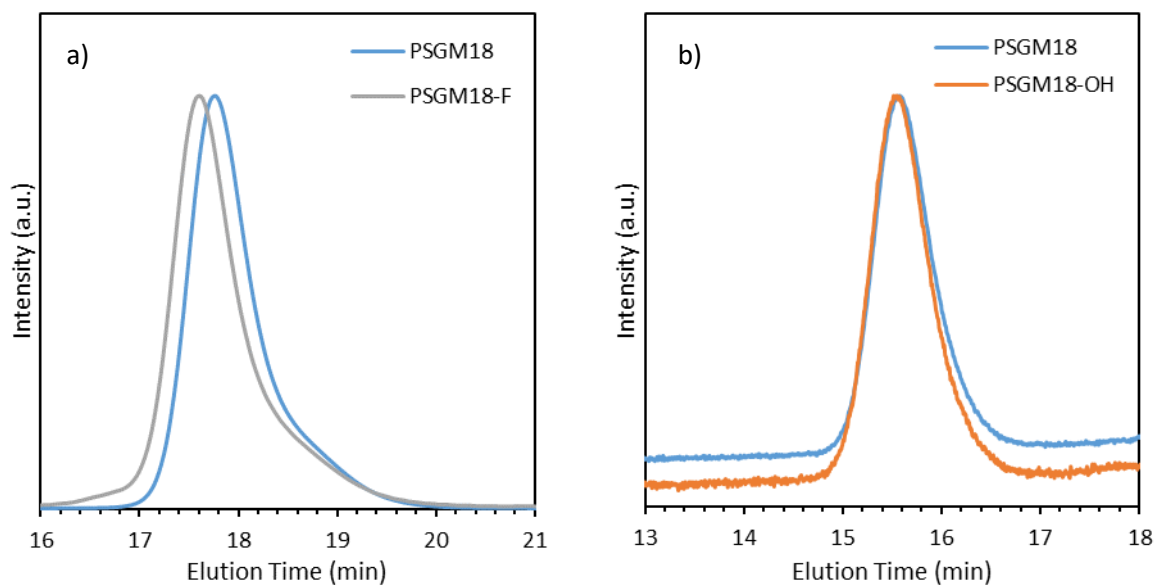


**Figure S6.** SEC traces of a) PSGM18 and PSGM18$_F$ in THF and b) PSGM18 and PSGM18$_{OH}$ in DMF.
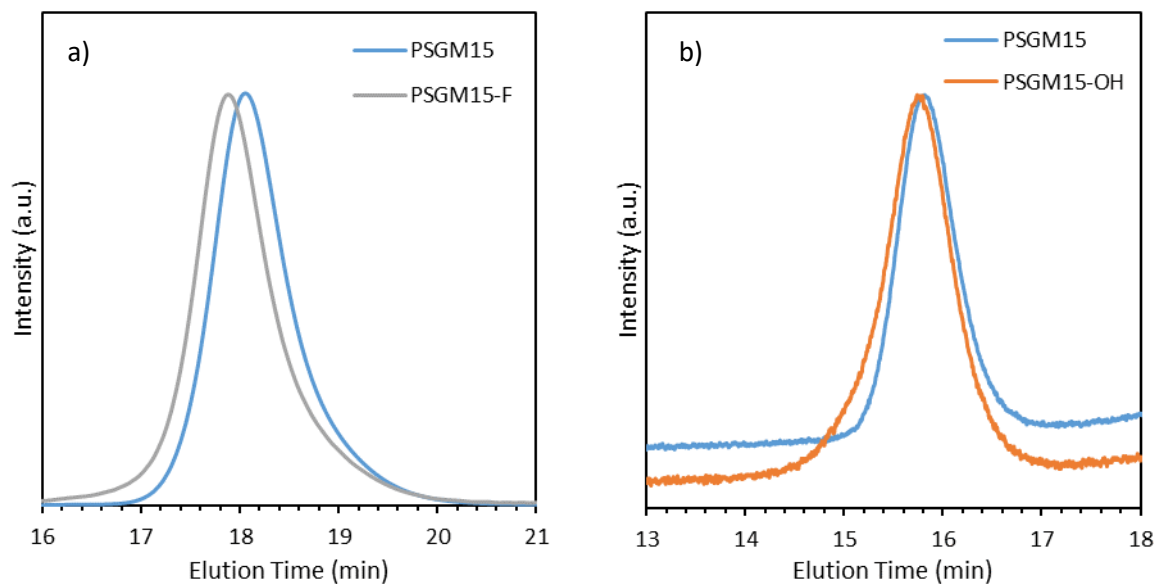
**Figure S7.** SEC traces of a) PSGM15 and PSGM15$_F$ in THF and b) PSGM15 and PSGM15$_{OH}$ in DMF.
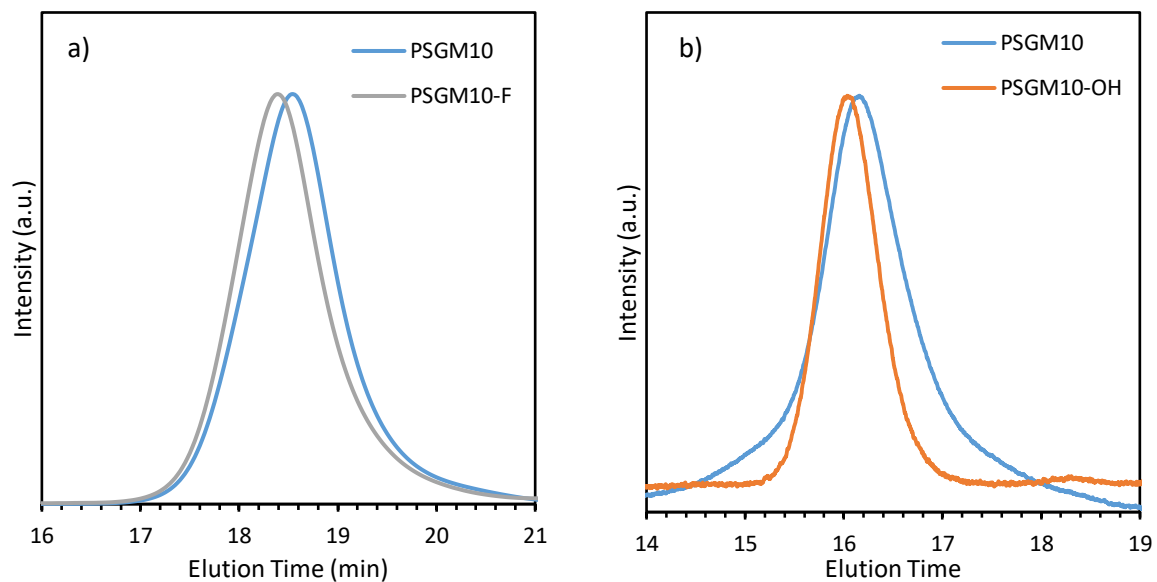


**Figure S8.** SEC traces of a) PSGM10 and PSGM10$_F$ in THF and b) PSGM10 and PSGM10$_{OH}$ in DMF.

**SAXS Thermal Experiments**

SAXS profiles were measured at reduced pressure at each temperature using a Bruker NanoSTAR (50 kV/ 50 mA) with a wavelength of 1.54 Å and a sample-to-detector distance of 1.0 m equipped with a TCPU-H heating stage and a Våntec-500 detector. Samples were placed in quartz glass capillaries (wall thickness 0.1 mm) for measurement. The SAXS profiles were collected using a cooling process beginning from 250 °C and cooled at a rate of 1 °C min^{-1}. At each measurement temperature, the sample was held for 15 min and exposed to X-ray radiation for 15 min to collect the spectrum. Background spectra were collected for each sample by exposing an empty glass capillary for 15 min. These background spectra were then subtracted from the experimental spectra to remove any potential scattering from the capillary or air scattering.

**Calculating $\chi$ using random phase approximation**

The temperature dependence of each pairwise $\chi$ parameter was calculated using the random phase approximation (RPA) by fitting the first order scattering peak of diblock or triblock copolymers in the disordered state over a range of temperatures. The fitting equations for RPA for a linear AB or ABC triblock are given by:[1–3]

$$I_{AA}(q) = K \frac{F_{AA}(q)}{\Delta(q)}$$

Where *K* is a proportionality constant which is unimportant in the fitting process and $F(q)$ is an expression which depends on all $\chi_{ij}$ and chain structure factors $S_{ij}$ for $(ijk) \in \{(ABC), (BCA), (CAB)\}$ and is given by:

$$F_{AA}(q) = C_{ABC}(q) - 2\chi_{AB}A(q)$$

where:

$$A(q) = S_{AA}(q)S_{BB}(q)S_{CC}(q) + 2S_{AB}(q)S_{AC}(q)S_{BC}(q)$$

$$-[S_{AC}^2(q)S_{BB}(q) + S_{BC}^2(q)S_{AA}(q) + S_{AB}^2(q)S_{CC}(q)]$$

$$C_{ABC} = S_{AA}(q)[S_{BB}(q) + S_{CC}(q) + 2S_{BC}(q)] - [S_{AB}(q) + S_{AC}(q)]^2.$$

The denominator is given by:

$$\Delta(q) = S(q) + \sum_{(ijk)} \left[ 2\chi_{ij}B_{ijk}(q) - A(q)(\chi_{ij}^2 - 2\chi_{ij}\chi_{ik}) \right]$$

where:

$$B_{ijk}(q) = S_{ij}^2(q) + S_{ij}(q)\left[S_{ik}(q) + S_{jk}(q) + S_{kk}(q)\right] - S_{ii}(q)S_{jj}(q) - S_{ii}(q)S_{jk}(q) -$$

$$S_{jj}(q)S_{ik}(q) - S_{ik}(q)S_{jk}(q).$$

For a linear block copolymer, the single chain structure factors are given by:

$$S_{ii}(q) = \frac{2\bar{N}f_i^2}{x_i^2}\left(x_i - 1 + [x_i(\lambda_i - 1) + 1]^{-(\lambda_i-1)^{-1}}\right) \text{ for } i \in \{A, B, C\}$$

$$S_{ij}(q) = \frac{\bar{N}f_if_j}{x_ix_j}\left(1 - [x_i(\lambda_i - 1) + 1]^{-(\lambda_i-1)^{-1}}\right)\left(1 - [x_j(\lambda_j - 1) + 1]^{-(\lambda_j-1)^{-1}}\right) \text{ for } ij \in \{AB, BC\}$$

$$S_{ik}(q) = \frac{\bar{N}f_if_k}{x_ix_k}\left(1 - [x_i(\lambda_i - 1) + 1]^{-(\lambda_i-1)^{-1}}\right)\left(1 - [x_k(\lambda_k - 1) + 1]^{-(\lambda_k-1)^{-1}}\right)\left([x_j(\lambda_j - 1) + 1]^{-(\lambda_j-1)^{-1}}\right) \text{ for } ik = AC \text{ and } j = B$$

where:

$$\bar{N} = \frac{\sum_i v_i N_i}{(\prod_i v_i)^{n^{-1}}}$$

$$x_i = \frac{N_{i,n}b_i^2}{6}q^2$$

$$\lambda_i = \lambda = \left(\frac{M_w}{M_n} - 1\right)\left(\sum_i w_i^2\right)^{-1} + 1$$

and $f_i$ is the volume fraction of the $i$th monomer, $v_i$ is the molar volume (in cm$^3$ mol$^{-1}$) of the $i$th monomer, $N_i$ is the degree of polymerization of the $i$th block, $N_{i,n}$ and $N_{i,w}$ are the number-average and weight-average molar masses of the $i$th block respectively, $\lambda_i$ is the dispersity of the $i$th block,

$b_i$ is the statistical segment length of the $i$th monomer (~0.68 nm for PS and ~0.74 nm for PMMA),[3] and $n$ is the number of different monomers (i.e. 2 for diblocks and 3 for triblocks). All degrees of polymerization were normalized to a reference volume of 118 Å$^3$.

The value of each pairwise interaction parameter were determined by the best fit of the scattering profile using the above equations at each temperature with the physical parameters listed in Table S1 and Table S2. For the diblock case, four parameters were fitted: $K$, $\chi_{AB}$, $b_A$, and $b_B$. For the triblock case, two of the three $\chi$ parameters were held constant at each temperature using their previously determined temperature dependencies and the following five parameters were fitted: $K$, $\chi$, $b_A$, $b_B$, and $b_C$. The temperature dependencies were then obtained by linear regression using the equation $\chi = \beta + \alpha T^{-1}$ where $\alpha T^{-1}$ is the enthalpic contribution and $\beta$ is the entropic contribution and $T$ is given in kelvin.

**Table S1.** Physical parameters of the polymers used for RPA analysis.

| Polymer Used | $M_n$ (kg mol$^{-1}$) | $f_A$ | $f_B$ | $f_C$ | $\lambda_A$ | $\lambda_B$ | $\lambda_C$ | $N_A$ | $N_B$ | $N_C$ |
|---|---|---|---|---|---|---|---|---|---|---|
| PS-PGMA-PMMA | 17.7 | 0.43 | 0.07 | 0.50 | 1.29 | 1.29 | 1.29 | 102 | 15 | 86 |
| PS-PGMA$_{OH}$-PMMA | 10.4 | 0.47 | 0.05 | 0.51 | 1.46 | 1.46 | 1.46 | 61 | 3 | 66 |
| PGMA$_{OH}$-PMMA | 4.0 | 0.43 | 0.57 | - | 1.36 | 1.36 | - | 10 | 35 | - |
| PS-PGMA$_F$-PMMA | 15.4 | 0.46 | 0.11 | 0.43 | 1.32 | 1.32 | 1.32 | 93 | 9 | 90 |

**Table S2.** Physical parameters of the monomers used for RPA analysis.

| Monomer | Molar Mass (g mol$^{-1}$) | Density (g cm$^{-3}$) | Molar Volume (cm$^3$ mol$^{-1}$) |
|---------|---------------------------|-----------------------|----------------------------------|
| Styrene | 104.15 | 1.05 | 99.2 |
| GMA | 142.15 | 0.805 | 177 |
| GMA$_{OH}$ | 250.31 | 1.50[a] | 167 |
| GMA$_F$ | 258.26 | 1.43[a] | 181 |
| MMA | 100.12 | 1.184 | 84.6 |

[a]Estimated using the group contribution method[4]
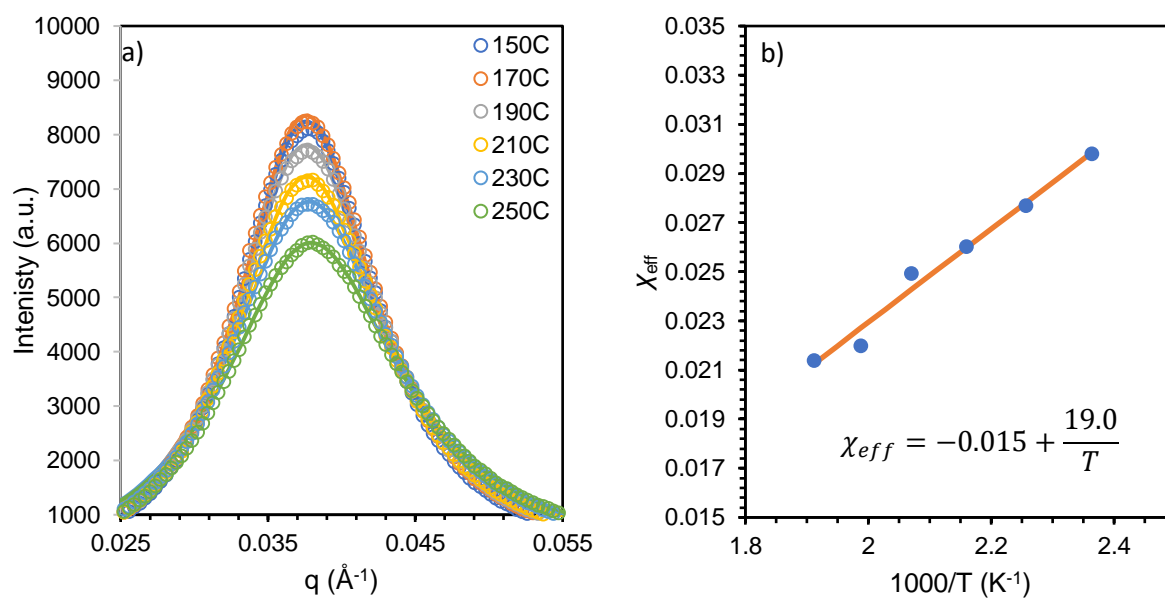


**Figure S9.** a) Fitting of PS-PGMA-PMMA using RPA and b) temperature dependence of $\chi_{GMA\text{-}MMA}$.

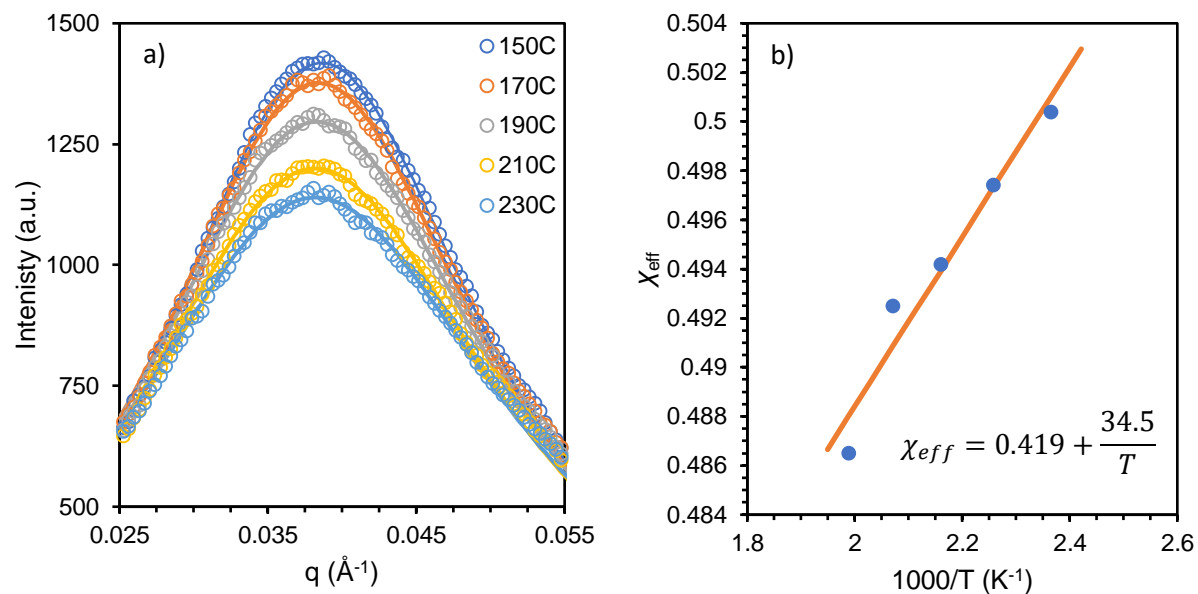$$\chi_{eff} = -0.015 + \frac{19.0}{T}$$

**Figure S10.** a) Fitting of PS-PGMA$_{OH}$-PMMA using RPA and b) temperature dependence of $\chi_{S\text{-}GMA\text{-}OH}$.



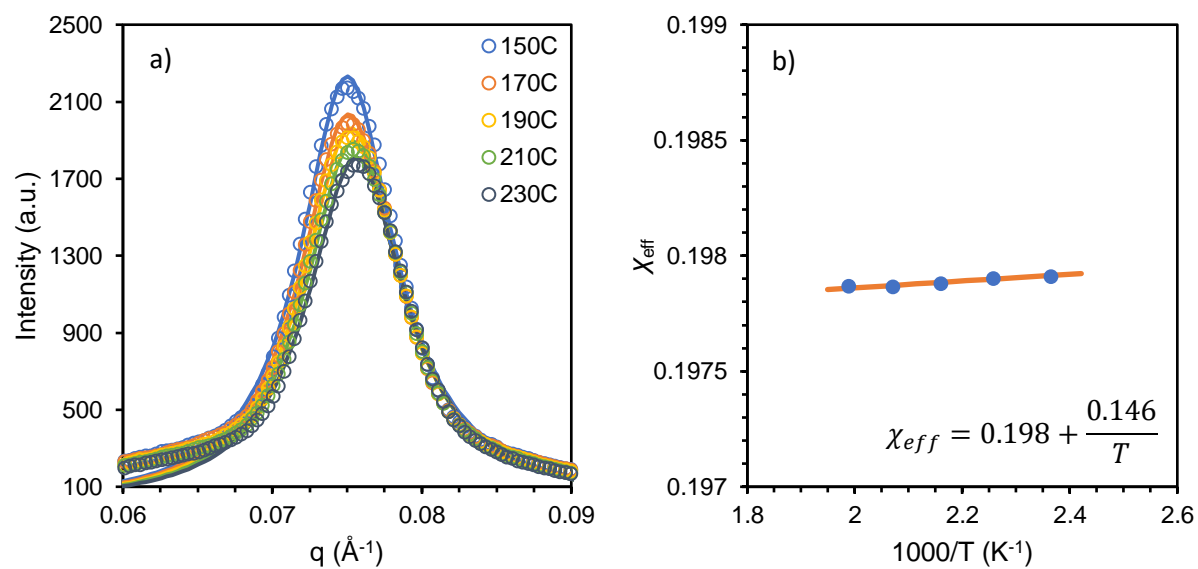**Figure S11.** a) Fitting of PGMA$_{OH}$-PMMA using RPA and b) temperature dependence of $\chi_{MMA\text{-}GMA\text{-}OH}$.
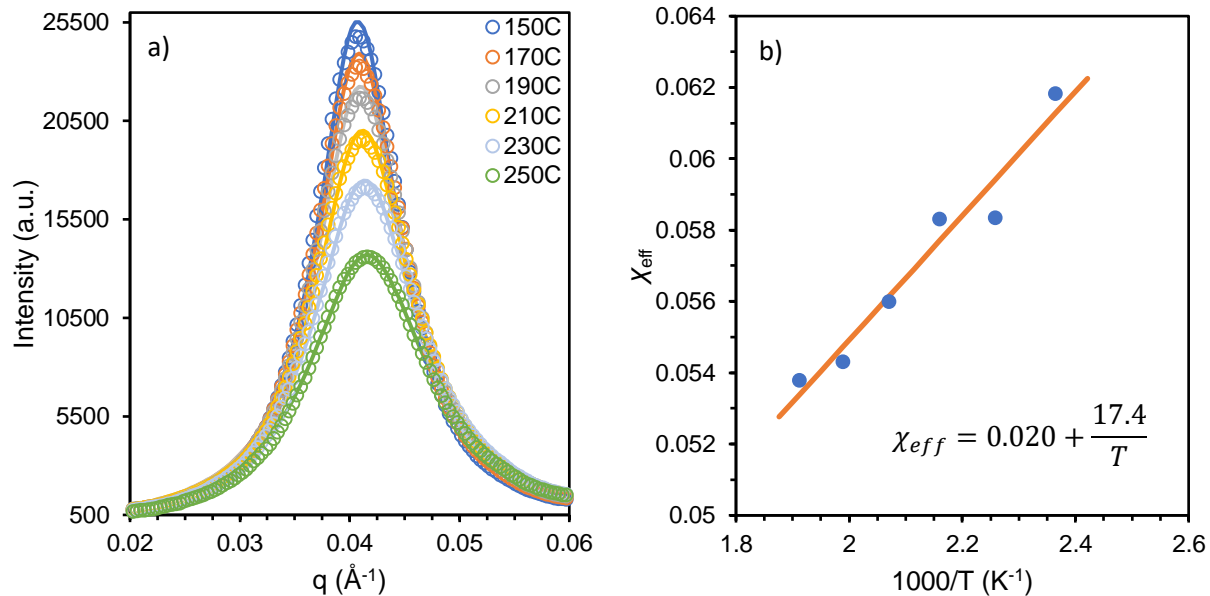
**Figure S12.** a) Fitting of PS-PGMA$_F$-PMMA using RPA and b) temperature dependence of $\chi_{\text{MMA-GMA-F}}$.

## SCFT Calculation of 2D Composition Profiles

The 2-dimensional volume fraction profiles for each monomer were obtained by SCFT simulation using the pseudo-spectral algorithm of Rasmussen and Kalosakas starting from random initial conditions.[5,6] The degree of polymerization and volume fractions of each polymer are shown in Table S3. $\chi_{\text{AB}}N$ and $\chi_{\text{BC}}N$ were systematically varied from 1 to 135 while four discrete $\chi_{\text{AC}}N$ values (4.94, 7.22, 8.64, and 10.1) were used to match the experimental $\chi N$ of each polymer studied. All of the simulated polymers were assumed to be monodisperse and have identical statistical segment lengths. A simulation box of size $L \times L$ with $L = 8\,R_{\text{g}}$ with periodic boundary conditions and a spatial resolution of $0.125\,R_{\text{g}}$ was used for all simulations. To accelerate the convergence of the simulation, Anderson acceleration was applied once changes in the free energy reached $\leq 1 \times 10^{-6}$.[7] Calculations were performed on an Intel Xeon CPU E5-2690V2 3.00 GHz or an Intel Xeon CPU Gold 6130 2.10 GHz.

13

**Table S3.** Input parameters for SCFT calculations.

| Simulated Sample Code | $f_A$ | $f_B$ | $f_C$ | Degree of Polymerization (N) | $\chi_{AC}$ |
|---|---|---|---|---|---|
| PSGM21 | 0.465 | 0.07 | 0.0465 | 267 | 0.0380 |
| PSGM18 | 0.45 | 0.1 | 0.45 | 227 | 0.0380 |
| PSGM15 | 0.45 | 0.1 | 0.45 | 190 | 0.0380 |
| PSGM10 | 0.475 | 0.05 | 0.475 | 130 | 0.0380 |

## 1D Composition Profiles

One dimensional composition profiles of several representative phases were computed in real-space using the finite-element Crank-Nicolson method.[8] As with the 2D simulations, statistical segment lengths are assumed to be equal and the results are expressed in units of $R_g$. Results were computed using a minimum spatial resolution of $\Delta r = 0.01$ and a minimum contour step of $\Delta s = 0.002$ using periodic boundary conditions and starting from random initial conditions.
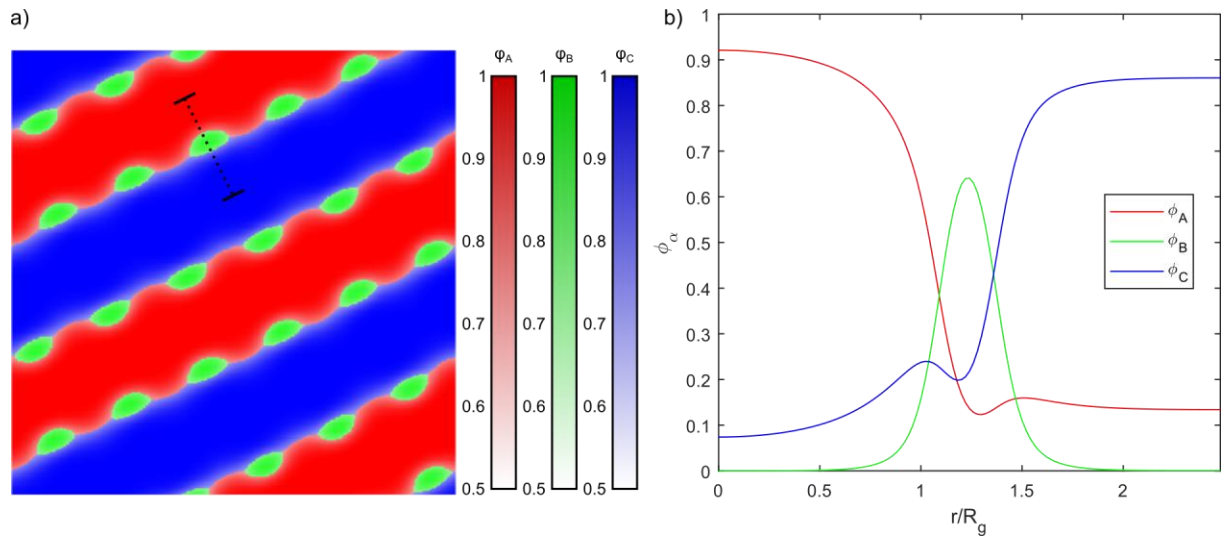


**Figure S13.** a) Morphology of PSGM21 *ls* phase calculated using SCFT at $\chi_{AB}N = 105$, $\chi_{BC}N = 120$ and $\chi_{AC}N = 10.14$ and b) 1D composition profile along the dotted line in units of $R_g$ calculated using $L = 2.5\ R_g$ with a contour step of $\Delta s = 0.002$ and a space step of $\Delta r = 0.01\ R_g$.
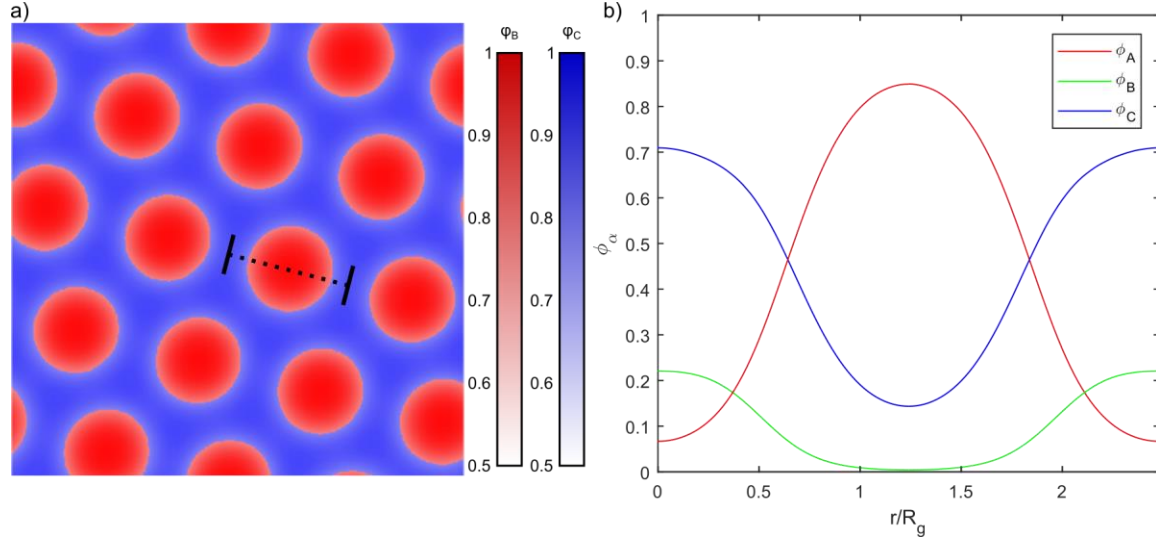
**Figure S14.** a) Morphology of PSGM21 HEX phase calculated using SCFT at $\chi_{AB}N = 90$, $\chi_{BC}N = 15$ and $\chi_{AC}N = 10.14$ and b) 1D composition profile along the dotted line in units of $R_g$ calculated using $L = 2.5 \, R_g$ with a contour step of $\Delta s = 0.002$ and a space step of $\Delta r = 0.01 \, R_g$.
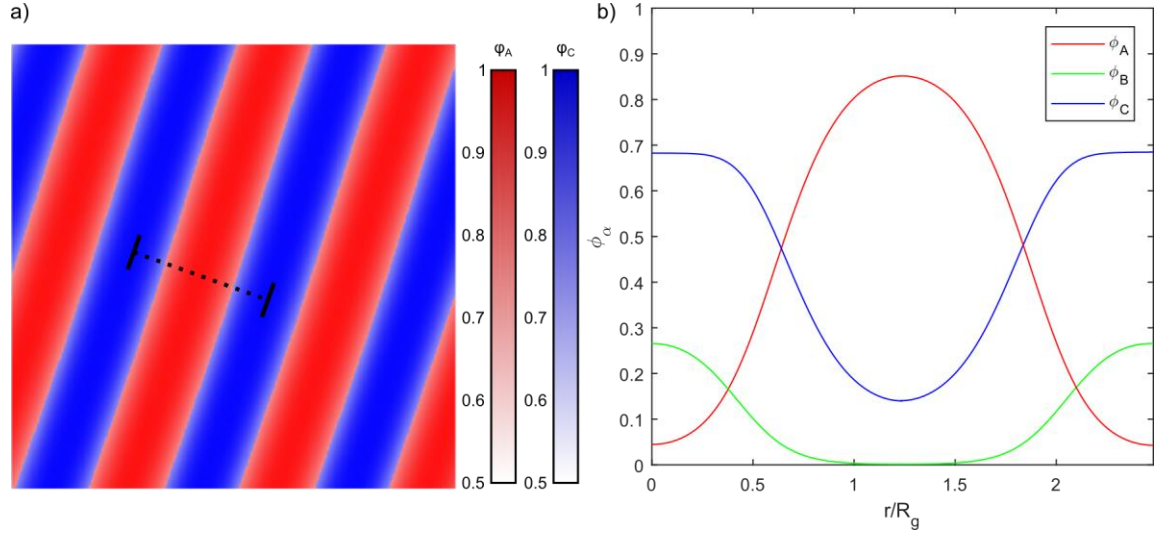


**Figure S15.** a) Morphology of PSGM21 LAM phase calculated using SCFT at $\chi_{AB}N = 135$, $\chi_{BC}N = 1$ and $\chi_{AC}N = 10.14$ and b) 1D composition profile along the dotted line in units of $R_g$ calculated using $L = 2.5 \, R_g$ with a contour step of $\Delta s = 0.002$ and a space step of $\Delta r = 0.01 \, R_g$.
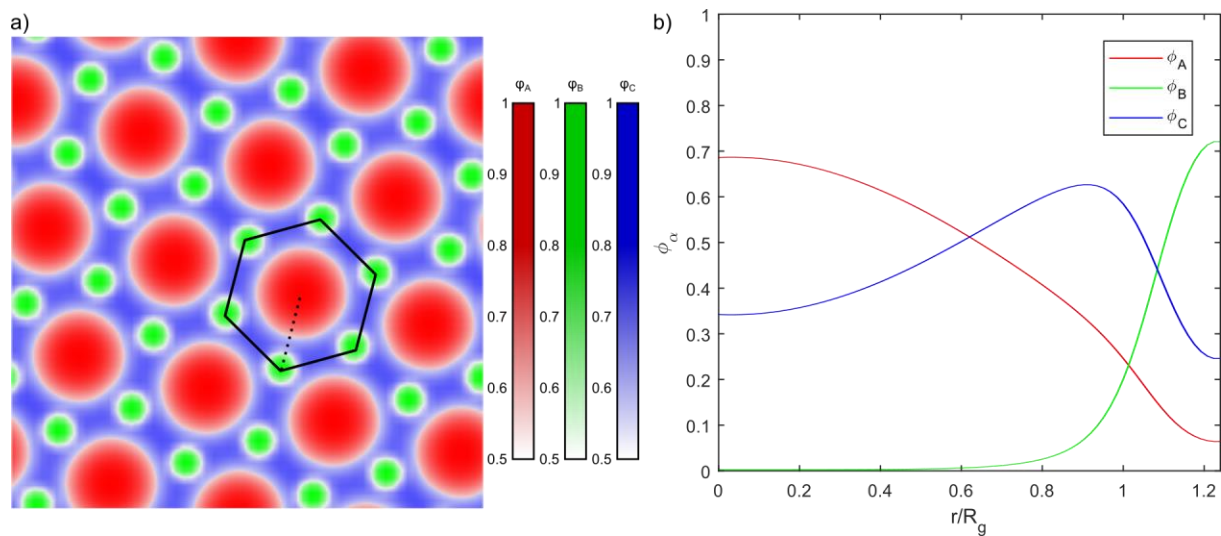
**Figure S16.** a) Morphology of PSGM18 c*s* phase calculated using SCFT at $\chi_{AB}N = 135$, $\chi_{BC}N = 90$ and $\chi_{AC}N = 8.64$ and b) 1D composition profile along the dotted line in units of $R_g$ calculated using $L = 1.25\ R_g$ with a contour step of $\Delta s = 0.002$ and a space step of $\Delta r = 0.005\ R_g$.
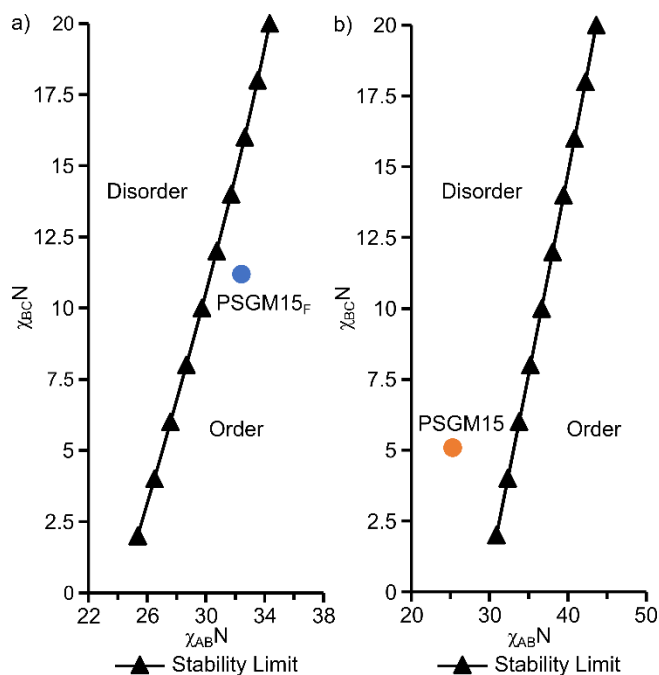


**Figure S17.** Calculation of the order-disorder transition with the RPA for a) PSGM15$_F$ and b) PSGM15 using the experimentally determined dispersity, normalized degree of polymerization, and volume fractions.

REFERENCES

(1)   Sakurai, S.; Mori, K.; Okawara, A.; Kimishima, K.; Hashimoto, T. Evaluation of Segmental Interaction by Small-Angle x-Ray Scattering Based on the Random-Phase Approximation for Asymmetric, Polydisperse Triblock Copolymers. *Macromolecules* **1992**, *25* (10), 2679–2691. https://doi.org/10.1021/ma00036a019.

(2)   Werner, A.; Fredrickson, G. H. Architectural Effects on the Stability Limits of ABC Block Copolymers. *Journal of Polymer Science Part B: Polymer Physics* **1997**, *35* (5), 849–864. https://doi.org/10.1002/(SICI)1099-0488(19970415)35:5<849::AID-POLB14>3.0.CO;2-A.

(3)   Zhao, Y.; Sivaniah, E.; Hashimoto, T. SAXS Analysis of the Order−Disorder Transition and the Interaction Parameter of Polystyrene-Block-Poly(Methyl Methacrylate). *Macromolecules* **2008**, *41* (24), 9948–9951. https://doi.org/10.1021/ma8013004.

(4)   Fedors, R. F. A Method for Estimating Both the Solubility Parameters and Molar Volumes of Liquids. *Polym. Eng. Sci.* **1974**, *14* (2), 147–154. https://doi.org/10.1002/pen.760140211.

(5)   Tzeremes, G.; Rasmussen, K. Ø.; Lookman, T.; Saxena, A. Efficient Computation of the Structural Phase Behavior of Block Copolymers. *Phys. Rev. E* **2002**, *65* (4), 041806. https://doi.org/10.1103/PhysRevE.65.041806.

(6)   Rasmussen, K. Ø.; Kalosakas, G. Improved Numerical Algorithm for Exploring Block Copolymer Mesophases. *Journal of Polymer Science Part B: Polymer Physics 40* (16), 1777–1783. https://doi.org/10.1002/polb.10238.

(7)   Thompson, R. B.; Rasmussen, K. O.; Lookman, T. Improved Convergence in Block Copolymer Self-Consistent Field Theory by Anderson Mixing. *J. Chem. Phys.* **2003**, *120* (1), 31–34. https://doi.org/10.1063/1.1629673.

(8)   Ackerman, D. M.; Delaney, K.; Fredrickson, G. H.; Ganapathysubramanian, B. A Finite Element Approach to Self-Consistent Field Theory Calculations of Multiblock Polymers. *J. Comput. Phys.* **2017**, *331*, 280–296. https://doi.org/10.1016/j.jcp.2016.11.020.